

Data-Augmented Numerical Integration in State Prediction: Rule Selection

J. Duník* L. Král* J. Matoušek* O. Straka* M. Brandner**

* Dept. of Cybernetics, ** Dept. of Mathematics
Univ. of West Bohemia, Univerzitní 8, 306 01 Pilsen, Czech Republic
e-mails: {dunikj,ladkral,matoujak,straka30}@kky.zcu.cz,
brandner@kma.zcu.cz

Abstract: This paper deals with the state prediction of nonlinear stochastic dynamic systems. The emphasis is laid on a solution to the integral Chapman-Kolmogorov equation by a deterministic-integration-rule-based point-mass method. A novel concept of reliable *data-augmented*, i.e., mathematics- and data-informed, integration rule is developed to enhance the point-mass state predictor, where the trained neural network (representing *data* contribution) is used for the selection of the best integration rule from a set of available rules (representing *mathematics* contribution). The proposed approach combining the best properties of the standard mathematics-informed and novel data-informed rules is thoroughly discussed.*

* This work has been submitted to IFAC for possible publication.

Keywords: State estimation, Neural network, Numerical integration, Nonlinear predictors, Bayesian methods, Stochastic systems.

1. INTRODUCTION

State estimation of nonlinear discrete-time stochastic dynamic systems from noisy or incomplete measurements has been a subject of considerable research interest for the last seven decades. Prediction can be understood as a task of estimating the future state with respect to the last available measurement. Thus, this task is essential in many applications ranging from signal processing and predictive control through navigation and economy to weather forecast. State prediction is also an inherent part of any filtering or smoothing algorithm (Särkkä, 2013), (Chen et al., 2015).

In this paper, the stress is laid on the state prediction of a system modeled by a nonlinear discrete-in-time stochastic dynamic model. In particular, the emphasis is put on the Bayesian approach, where the predictive (conditional) probability density function (PDF) of the state is calculated. A general solution to the prediction is given by the *integral* Chapman-Kolmogorov equation (CKE).

1.1 Related Work

The CKE is exactly solvable for a limited set of dynamic models, for which the linearity and Gaussianity are usually common factors (Särkkä, 2013; Stroud, 1971). In other cases, i.e., for nonlinear or non-Gaussian models, an approximate solution to the CKE is employed. The approximate solutions to the CKE for a nonlinear model either (i) linearize the model or apply the numerical integration rules, or (ii) utilize a machine learning method for approximation of the numerical solution or the prediction.

Mathematical-driven Methods The first group of approximate methods is based on the linearization of the involved

nonlinear functions in the dynamics and assumption of a Gaussian PDF of all related random variables, which allows to apply the solution to the CKE known for the linear and Gaussian model. Often, linearization techniques based on the Taylor expansion, Stirling's interpolation, or statistical linearization are used, and the resulting prediction is in the form of the mean and covariance matrix (Julier and Uhlmann, 2004; Šimandl and Duník, 2009; Särkkä, 2013). The *second* group solves the integral CKE by various numerical integration rules (IRs). In the literature, two groups of methods can be found, namely density-specific and grid-based. Whereas the density-specific methods rely on the assumption of certain forms of the integrated PDFs (e.g., Gaussian, Student's-t) (Julier and Uhlmann, 2004; Šimandl and Duník, 2009; Duník et al., 2015), the grid-based methods cover the state-space by a grid of deterministically or randomly placed points used for the integral solution. The popular integration methods are represented by, e.g., Monte-Carlo methods or the midpoint rule (Stroud, 1971; Doucet et al., 2001; Closas et al., 2009; Särkkä, 2013), (Duník et al., 2022). To achieve higher accuracy, the Richardson extrapolation or the Newton-Cotes formulas, such as a trapezoid or Simpson rule, can be applied (Stoer et al., 2002). For multiple-dimensional integration, the IRs for the specific dimensions are proposed as an alternative to a combination of one-dimensional rules (Miller, 1960). Besides the above-mentioned deterministic IRs with the equidistantly spaced integration nodes, the adaptive IRs with non-equidistantly spaced grid can also be used. The adaptive rules might provide better performance (Press et al., 2007), but usually at the cost of higher computational complexity. Note that the methods of this group are also suitable for linear models with a non-Gaussian prior PDF.

Application of these integration methods has led to a plethora of predictors ranging from rather simple ones utilizing the prediction step of the local filters, such as the extended or unscented Kalman filter, to more advanced global ones being based on the particle or point-mass filters (Šimandl and Duník, 2009; Särkkä, 2013). The methods have been thoroughly analyzed with regard to convergence and integration errors.

Data-driven Methods Recently, the advancement in machine learning has enabled the design of the *second* group of integration methods, i.e., of the *data-driven* integration rules (Zhe-Zhao et al., 2006; Lloyd et al., 2020; Yoon, 2021; Alsadi et al., 2023). These rules solve the integral relations using the pre-trained neural networks (NN). Indeed, the integral can be seen as a transformation of an integrand to an integration result, and as any other transformation (or function), it can be completely substituted by the NN (end-to-end approach). Note that the approaches considered have a major limitation: the assumption of fixed integration. As such, they are *not* suitable in the considered problem of the CKE solution since the integrand varies at each time instant of state estimation (due to the time evolution of the PDF). Besides the area of numerical integration, the NNs have been directly used in the state estimator design for more than two decades. Originally, the NNs were used for system modeling with or without respecting the physics behind (Gorji and Menhaj, 2008; Bao et al., 2020; Schoukens, 2021). These models were then used in the estimation or prediction algorithms discussed above. Then, the NNs have been used directly at the level of estimation algorithms, i.e., to replace the prediction or estimation algorithms with the NN without the need for a model knowledge (Zhai et al., 2019; Shaukat et al., 2021; Heo and Lee, 2018; Zhai et al., 2019; Tian et al., 2020; Alsadi et al., 2023). Compared to the mathematics-driven methods, the NN-based approaches do not require any deep insight into the solved task. On the other hand, the NN has to be well (or life-long) trained to provide reliable results, which cannot be analytically assessed in terms of integration output properties. NN training is typically time and computationally demanding.

1.2 Motivation and Paper Contribution

Irrespectively to which method is used for an approximate CKE solution, the calculated predictive PDF is inherently associated with an *integration error*, and the selection of the suitable IR with required properties remains *difficult* and *problem specific* task with no globally valid guidelines. Ultimately, the IR selection is left to the predictor designer or user, who is expected to possess a deeper insight into the solved task and knowledge of a wide range of data and mathematics-driven numerical methods.

The *goal* of the paper is to propose, validate, and illustrate an innovative concept of *data-augmented* IR enhancing a numerical-IR-based state predictor with an NN. Instead of designing another numerical IR, state predictor, or its NN-based counterpart, we exploit the developed and thoroughly analyzed IRs and supplement them with a pre-trained NN classifier that is able to select the “best” IR for the considered task and working conditions at each time instant. The data-augmented IR, thus, combines the

desired properties of the *mathematics-informed* IR, such as error analysis and convergence rate and *data-informed* IR with an ability to find hidden relations between working conditions and IR performance.

In this paper, we design the data-augmented IR based on the *selection* of the most suitable IR by the NN for the CKE solution in actual working conditions. The stress is laid on the descriptor specification and analysis of the proposed data-augmented integration rule error. The proposed IR *minimizes* the user or designer interaction to obtain sufficiently precise IR error estimates, which, in the end, improves the accuracy of the state prediction with minimal impact on computational complexity.

The proposed concept is analyzed and illustrated using the popular *grid-based deterministic IRs* and the state prediction using the *point-mass method* (PMM) widely used in signal processing and navigation applications (Bergman, 1999; Šimandl et al., 2006; Lindfors et al., 2016; Jeon et al., 2018; Duník et al., 2019). It can be, however, extended for any other numerical methods. Source code in MATLAB of the data-augmented IR is publicly available.

2. SYSTEM DEFINITION AND STATE PREDICTION

A system with dynamics described by the discrete-time nonlinear stochastic difference state equation

$$\mathbf{x}_{k+1} = \mathbf{f}_k(\mathbf{x}_k, \mathbf{u}_k) + \mathbf{w}_k \quad (1)$$

is considered, where $\mathbf{x}_k \in \mathbb{R}^{n_x}$ is the sought state of the system, $\mathbf{u}_k \in \mathbb{R}^{n_u}$ is the known input, and $\mathbf{w}_k \in \mathbb{R}^{n_x}$ is the unknown state noise at time k . The nonlinear function $\mathbf{f}_k : \mathbb{R}^{n_x \times n_u} \rightarrow \mathbb{R}^{n_x}$ is known as well as the PDF¹ of the noise $p(\mathbf{w}_k)$.

Given “initial²” PDF $p(\mathbf{x}_k)$, the “predictive” PDF $p(\mathbf{x}_{k+1})$ can be computed by the CKE as

$$p(\mathbf{x}_{k+1}) = \int p(\mathbf{x}_{k+1}|\mathbf{x}_k)p(\mathbf{x}_k)d\mathbf{x}_k, \quad (2)$$

where $p(\mathbf{x}_{k+1}|\mathbf{x}_k) = p_{\mathbf{w}_k}(\mathbf{x}_{k+1} - \mathbf{f}_k(\mathbf{x}_k, \mathbf{u}_k))$ is the transition PDF obtained from (1).

Considering the nonlinear function \mathbf{f}_k or non-Gaussian PDFs $p(\mathbf{x}_k)$ and $p(\mathbf{w}_k)$, the CKE (2) is not analytically tractable and an approximate solution, numerical PMM based on the midpoint IR in this case, is used.

2.1 CKE Solution by Numerical Integration Rules

Standard numerical solution to the CKE (2) by the PMM starts with the approximation of the initial PDF $p(\mathbf{x}_k)$ by the *piece-wise* constant point-mass density (PMD) (Bergman, 1999; Šimandl et al., 2006; Duník et al., 2019) defined at the set of the discrete grid points $\Xi_k = \{\xi_k^{(i)}\}_{i=1}^N, \xi_k^{(i)} \in \mathbb{R}^{n_x}$ (in a rectangular and equidistant grid), which are in the center of their respective non-overlapping neighborhood $\Delta_k^{(i)}$

$$p(\mathbf{x}_k) \approx \hat{p}(\mathbf{x}_k; \Xi_k) \triangleq \sum_{i=1}^N p_k(\xi_k^{(i)}) S\{\mathbf{x}_k; \xi_k^{(i)}, \Delta_k^{(i)}\}, \quad (3)$$

¹ For the sake of notational convenience, a PDF $p_{\mathbf{w}_k}(\mathbf{w}_k)$ is denoted as $p(\mathbf{w})$, if it does not lead to ambiguity.

² In the state estimation concept, the initial PDF can be either the filtering PDF or predictive PDF from previous time instant.

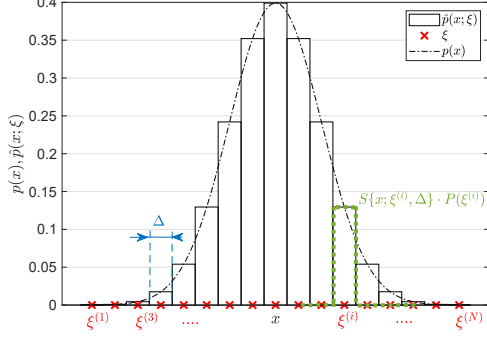


Fig. 1. Illustration of point-mass PDF approximation (grid points - red, grid point neighborhood - blue, selection function - green).

where $N = N_1 \cdot N_2 \dots \cdot N_{n_x}$, and N_i is a number of discretization points in i -th dimension of the state \mathbf{x}_k , $p_k(\boldsymbol{\xi}_k^{(i)}) = p(\mathbf{x}_k^{(i)})$ is the value of the PDF $p(\mathbf{x}_k)$ evaluated at the i -th grid point $\mathbf{x}_k^{(i)}$ further also called as a *weight* (the PMD is normalized to integrate to 1), $\Delta_k^{(i)}$ is rectangular grid cell centered at $\boldsymbol{\xi}_k^{(i)} \in \mathbb{R}^d$ with the volume δ_k , where $\hat{p}(\mathbf{x}_k; \Xi_k)$ is constant, and $S\{\mathbf{x}_k; \boldsymbol{\xi}_k^{(i)}, \Delta_k\}$ is an indicator function that equals to 1 if $\mathbf{x}_k \in \Delta_k^{(i)}$. Illustration of the point-mass PDF approximation (3) for $n_x = 1$ with omitted time indices is shown in Fig. 1.

Then, a significant part of the predictive PDF $p(\mathbf{x}_{k+1})$ support³ is covered by a set of the *predictive* grid points $\Xi_{k+1} = \{\boldsymbol{\xi}_{k+1}^{(j)}\}_{j=1}^N$ and the predictive PMD solving (2) becomes

$$\hat{p}(\mathbf{x}_{k+1}; \Xi_{k+1}) = \sum_{j=1}^N p_{k+1}(\boldsymbol{\xi}_{k+1}^{(j)}) S\{\mathbf{x}_{k+1}; \boldsymbol{\xi}_{k+1}^{(j)}, \Delta_{k+1}\}, \quad (4)$$

where

$$p_{k+1}(\boldsymbol{\xi}_{k+1}^{(j)}) = \int p(\boldsymbol{\xi}_{k+1}^{(j)} | \mathbf{x}_k) p(\mathbf{x}_k) d\mathbf{x}_k. \quad (5)$$

2.2 Numerical Integration and its Error

Considering the initial PDF $p(\mathbf{x}_k)$ in the form of the PMD (3), the integral CKE (5) is typically evaluated using the standard *midpoint* IR given by (Bergman, 1999)

$$\hat{P}_{k+1}^M(\boldsymbol{\xi}_{k+1}^{(j)}) = \sum_{i=1}^N p(\boldsymbol{\xi}_{k+1}^{(j)} | \mathbf{x}_k = \boldsymbol{\xi}_k^{(i)}) P_{k|k}(\boldsymbol{\xi}_k^{(i)}) \delta_k. \quad (6)$$

The standard approach uses the Richardson extrapolation of the midpoint rule (Herman and Strang, 2017) to achieve higher integration accuracy. The extrapolation calculates the midpoint IR twice while changing integration node density, i.e., Δ_k . Let $K(\Xi_k; \Delta_k)$ be an integration rule with integration nodes distance Δ_k (e.g., (6)), and $K(\Xi_k; 2\Delta_k)$ with doubled distance, i.e., every second grid point is used for the calculation. Then, the value of the predictive PDF at j -th grid point reads

³ The predictive PDF support can be found using a fast linearization based on the Taylor expansion or the unscented transform (Anderson and Moore, 1979; Julier and Uhlmann, 2004; Bergman, 1999).

$$\hat{P}_{k+1}^R(\boldsymbol{\xi}_{k+1}^{(j)}) = K(\Xi_k; \Delta_k) + \frac{1}{2^o - 1} [K(\Xi_k; \Delta_k) - K(\Xi_k; 2\Delta_k)], \quad (7)$$

where $o = 2$ is the order of the midpoint IR.

Except for a few cases, the output of all numerical IRs, e.g., of (6), (7), is subject to an error. Thus, the value of the predictive PDF (5) can be rewritten as

$$p_{k+1}(\boldsymbol{\xi}_{k+1}^{(j)}) = \hat{P}(\boldsymbol{\xi}_{k+1}^{(j)}) + \varepsilon_{k+1}(\boldsymbol{\xi}_{k+1}^{(j)}), \quad (8)$$

where $\varepsilon_{k+1}(\boldsymbol{\xi}_{k+1}^{(j)})$ is an IR-induced error and $\hat{P}(\boldsymbol{\xi}_{k+1}^{(j)})$ is an approximation of integral (5) computed by a chosen IR, e.g., (6), (7).

2.3 Motivation Example and Goal of the Paper

The midpoint IR with the Richardson interpolation generally overcomes the standard midpoint rule (regarding the maximal error). However, for certain cases, the midpoint rule can have an actual error smaller than the interpolated IR, making the rule selection inherently complicated. This situation is illustrated using a system with *non-Gaussian* initial PDF and linear dynamics (1)

$$f_k(x_k) = Fx_k \quad (9)$$

where $F = 1$, $n_x = 1$, and $p(w_k) = \mathcal{N}\{w_k; 0, Q\}$, with $Q = 2$. The notation $\mathcal{N}\{\mathbf{x}; \hat{\mathbf{x}}, \Sigma_x\}$ stands for the Gaussian PDF of a random variable \mathbf{x} with the mean $\hat{\mathbf{x}} = E[\mathbf{x}]$ and covariance matrix $\Sigma_x = \text{cov}[\mathbf{x}]$. Further, let the initial PDF be in the form of the Gaussian sum (GS) PDF

$$p(x_k) = \sum_{g=1}^G \alpha_k^{(g)} \mathcal{N}\{x_k; \hat{x}_k^{(g)}, \Sigma_{x,k}^{(g)}\}, \quad (10)$$

where $\alpha_k^{(i)}$ is a weight of the i -th element $\mathcal{N}\{x_k; \hat{x}_k^{(i)}, \Sigma_{x,k}^{(i)}\}$ conveniently abbreviated as $\mathcal{N}^{(i)}\{x_k\}$. The initial and predictive grids Ξ_k and Ξ_{k+1} , respectively, have been designed with $N = 30$ grid points covering part of the state-spaces $\mathcal{S}_k = [\hat{x}_k - \sigma S_{x,k}, \hat{x}_k + \sigma S_{x,k}]$ and $\mathcal{S}_{k+1} = [\hat{x}_{k+1} - \sigma S_{x,k+1}, \hat{x}_{k+1} + \sigma S_{x,k+1}]$, respectively, where $S_{x,k} = \sqrt{\Sigma_{x,k}}$ and $\sigma = 6$.

In total $M = 6 \times 10^4$ Monte-Carlo (MC) simulations have been performed and the value of the predictive PDF $p(\mathbf{x}_{k+1})$ at the grid middle point $\boldsymbol{\xi}_{k+1}^{(j)}$ with⁴ $j = 15$ has been computed

- Exactly, denoted as $p(\boldsymbol{\xi}_{k+1}^{(15)})$,
- Numerically using the midpoint rule (6),
- Numerically using the midpoint rule with the Richardson extrapolation (7) with $o = 2$.

The properties of the initial PDF (10) were generated randomly using MC simulations, namely

- Number of terms G from the discrete uniform distribution with lower bound one and upper bound ten, i.e., from $\mathcal{U}\{1, 10\}$,

⁴ The considered grid point with $j = 15$ lies at the center of the grid Ξ_{k+1} and is often associated with a significant value of the PDF. Thus, a non-negligible difference between the outputs of different IRs can be observed, which is convenient for the motivation. Selection of the particular point does *not* affect the approach's generality, as illustrated later in numerical experiments.

Table 1. Accuracy of baseline IRs.

	Midpoint	Richardson	Best sel.
RMSE $\times 10^{-3}$	6.61	13.7	4.85
MARE [%]	6.1	19.3	4.9
Superiority	46082	13918	–

- Gaussian term mean $\hat{\mathbf{x}}^{(i)}$ from continuous uniform density $\mathcal{U}\{-5, 5\}$,
- Gaussian term variance $\mathbf{P}_x^{(i)}$ from continuous uniform density $\mathcal{U}\{0.1, 1\}$.

The performance of the numerical solutions has been validated using three criteria, namely

- Root-mean-square-error

$$\text{RMSE} = \sqrt{\frac{1}{M} \sum_{m=1}^M \left(\varepsilon_{k+1}(\boldsymbol{\xi}_{k+1}^{(15)}) \right)^2}, \quad (11)$$

- Mean absolute relative error

$$\text{MARE} = \frac{1}{M} \sum_{m=1}^M \text{abs} \left(\frac{\varepsilon_{k+1}(\boldsymbol{\xi}_{k+1}^{(15)})}{p(\boldsymbol{\xi}_{k+1}^{(15)})} \right), \quad (12)$$

where the function $\text{abs}(\cdot)$ means the absolute value,

- Superiority of the considered IRs, meaning the portion of the MC simulations in which given IR provides smaller RMSE.

The midpoint rule and Richardson interpolation results can be found in Table 1. Besides the results for the midpoint and extrapolated midpoint IRs, the “best” selective IR is given, which indicates the accuracy when the best rule is selected in each MC simulation. This best selective IR is a theoretical one, which can be computed if the exact value $p(\boldsymbol{\xi}_{k+1}^{(15)})$ (5) is known. The results indicate that the IR choice significantly affects the integration accuracy, and the integration error can be reduced with a suitable selection of the IR. It is worth noting that the theoretically better (Richardson) interpolation IR provides an error smaller than the simple midpoint rules in ca. a quarter of MC simulations only. The MC differs in the shape of the initial PDF only, and there is no theoretical justification for this behavior (or prediction of it), which would allow the selection of the best rule.

It means that the IR selection is *not* a trivial task (it depends on multiple characteristics of the input variables), and it is problem-specific. Selection of the IR based on the IR maximum error can also be misleading as it is typically based on assessment of the maximal error, whereas the actual error might be very different. Thus, it appears that the selection of appropriate IRs can be addressed by machine learning techniques, namely the NNs, which might extract some hidden dependencies between the model (9), initial PDF (10), and the IR rule error.

The *goal* of the paper is to propose and validate a novel concept of the data-augmented IR design for enhancement of the PMM prediction by the NN-based IR selection.

3. DATA-AUGMENTED IR SELECTION

The main motivation behind this approach is to consider the error magnitude of the IRs when designing the classi-

fier. The key point is first to find an estimate of the IR error using NNs, as shown in Fig. 2. Subsequently, an optimal IR is selected from B candidate IRs (e.g., midpoint and medpoint with the Richardson extrapolation) at each time instant according to

$$\mathcal{B}^* = \arg \min_b \text{abs} \left(\hat{\varepsilon}_{k+1}^{(b)}(\boldsymbol{\xi}_{k+1}^{(j)}) \right), b = 1, 2, \dots, B, \quad (13)$$

where instead of the true IR error $\varepsilon_{k+1}^{(b)}(\boldsymbol{\xi}_{k+1}^{(j)})$ its NN-based estimate $\hat{\varepsilon}_{k+1}^{(b)}(\boldsymbol{\xi}_{k+1}^{(j)})$ is used. The value of the integral calculated using the rule selected by the NN is denoted as $P_{k+1}^S(\boldsymbol{\xi}_{k+1}^{(j)})$. The error *estimator* can be trained using supervised learning to *minimize* the mean square error of the difference between the IR error $\varepsilon_{k+1}(\boldsymbol{\xi}_{k+1}^{(j)})$ and its estimate $\hat{\varepsilon}_{k+1}(\boldsymbol{\xi}_{k+1}^{(j)})$.

3.1 NN Structure and Training Features

As indicated by the analysis, the classification task is a non-trivial problem. Since no single form of the classifier is suitable for all data sets, an extensive set of methods has been developed during the last decades, including naive Bayesian, support vector machines, decision trees, and NNs (Saravanan and Sujatha, 2018). A NN-based classifier will be preferred due to its high versatility, efficiency, and performance.

An NN is defined by its structure, i.e., number of neurons, activation function type, number of layers, and topology (Haykin, 1999). Unfortunately, there is no fail-proof procedure for choosing the structure of the NN, and this option depends on the problem at hand. Thus, an appropriate choice of the NN structure will be described for a specific example in Section 4.

Independently of the NN structure, training features and evaluation criteria must be carefully selected. Principally, two different sets of features describing the initial PMD $\hat{p}(\mathbf{x}_k; \boldsymbol{\Xi}_k)$ (3) were considered:

- *Statistical*, characterising the PMD by the number of grid points N and a set of raw and central moments,
- *Analytical*, characterizing the PMD by the *first* and *second*-order central differences at considered grid points.

Both sets were supplemented with the PMD $\hat{p}(\mathbf{x}_k; \boldsymbol{\Xi}_k)$, grid points $\boldsymbol{\Xi}_k$, and the predictive grid point $\boldsymbol{\xi}_{k+1}^{(j)}$. Numerical experiments revealed that the statistical characteristics of the PMD have little effect on NN training and decision; thus, the analytical ones are preferred in this paper. The analytical features describe the *spatial* behavior of the PMD, which significantly affects the IR accuracy.

Regarding the evaluation criteria, the *classifier* was trained using cross-entropy as the loss function for the classification task with B mutually exclusive classes. The output of the NN classifier is the index \mathcal{B} of the selected IR.

3.2 Data-augmented IR Error Properties and NN (Re)training

The proposed data-augmented IRs generally benefit from the well-developed theory of stability, convergence, and

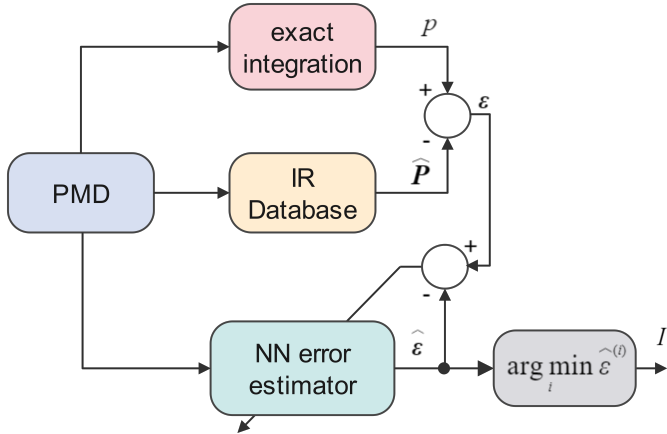


Fig. 2. Training process of NN error estimator.

error properties of the mathematics-driven IRs (Anthony and Rabinowitz, 1978; Zwillinger, 2003). Such property might be essential, e.g., from a certification perspective of a safety-critical system. Moreover, the data-augmented approach can also be used if no or a limited number of data is available. In such a case, the approach simply becomes the mathematics-driven one. The worst-case properties are driven by the least accurate numerical IR properties. The NN classifier needs to be repeated if a new IR is considered.

4. NUMERICAL ILLUSTRATION

The performance of the NN-enhanced PMM prediction is illustrated using the set-up defined in the motivation by (9), (10). The linear model with the GS initial PDF allows *exact* integral evaluation and, thus, exact calculation of the predictive PDF.

4.1 IR Selection

The experiment starts with a classification task where the best IR is selected out of the standard midpoint IR (6) and the midpoint IR with the Richardson extrapolation (7).

The details of the training process can be summarized as follows:

- **Data collection:** The data was generated using 10^6 evaluations of the integral “true” $p(\xi_{k+1}^{(j)})$ (5) and two numerical approximations $P_{k+1}^M(\xi_{k+1}^{(j)})$ (6) and $P_{k+1}^R(\xi_{k+1}^{(j)})$ (7).
- **Data pre-selection:** To improve the convergence rate of the NN training process and performance of the NN classifier/estimator, the data observations were pre-selected and only important ones were kept, i.e., those fulfilling $\varepsilon_{k+1}(\xi_{k+1}^{(j)}) > \beta$, where β is a threshold derived from the expected or typical magnitude of the processed initial PDF $p(x_k)$. In this experiment, $\beta = 10^{-2}$ is approximately 5% of the maximum value of the observed PDFs. Compensation for lower IR errors does not bring any benefit. Then, the IR value can be classified/compensated if the IR error is greater than the threshold.
- **Data cross-validation:** Data was divided into a training set (80%) and a test set (20%) for validation purposes.

Table 2. Accuracy of selective IRs (continuation of Table 1).

	Best	Selective IR
RMSE $\times 10^{-3}$	4.85	4.98
MARE [%]	4.9	5.0
Accuracy [%]	100	95.8

- **NN structure selection:** A feed-forward network with 87 identical inputs as in the previous case, followed by three fully connected layers with 128, 64, and 2 neurons with hyperbolic tangent activation functions, where the output of the last layer provides estimates of both IR errors. In this case, the total number of parameters is 19650.
- **NN parameter optimization:** The NN parameters were optimized using stochastic gradient descent with momentum (SGDM) algorithm with default/recommended learning rate parameters.

The pre-trained NN classifiers were used for the integral evaluation, where additional 10^4 observations were generated. The results can be seen in Table 2 w.r.t. RMSE (11), MARE (12), and accuracy, which gives a ratio of correct determination of the IR with a lower error.

The table indicates that the selective IR is only slightly worse than the best selective IR, which takes advantage of the availability of the true value of the integral. Analysis of this behavior revealed that the Richardson extrapolation leads to large errors in certain cases. Thus, a correct classification is required in such cases (i.e., not selection of the Richardson extrapolation).

4.2 PMM Prediction Step Error

In the previous parts, the predictive PDF was evaluated at a single point $\xi_{k+1}^{(j)}$, $j = 15$, only. However, to compute the predictive PMD, the convolution (4) has to be evaluated $\forall j$. For this purpose, the single NN for the midpoint rule has been retrained for all possible grid points $\xi_{k+1}^{(j)}$ with the same settings as specified in the motivation example in (9), (10). The standard and NN-based compensated midpoint IRs were validated using MARE criterion (12). The midpoint rule led to a criterion value of 16.2%, whereas **selective IR led to** value of 6.1%.

An exemplary source code in MATLAB illustrating NN structure and training for IR error estimation is available. The code requires Deep Learning Toolbox[©]. The source code is written to be easily modifiable in terms of considered dynamics⁵ (linear and nonlinear) and the state noise properties (<https://idm.kky.zcu.cz/files>).

5. CONCLUDING REMARKS

The paper dealt with a numerical solution to the Chapman-Kolmogorov equation by the point-mass method. The stress was laid on improving the numerical integration schemes by properly trained neural networks. The concept of the data-augmented, i.e., data and mathematics theory based, IR was proposed, where the best IR for the actual

⁵ According to the simulations, the data-augmented IR improvement is not affected by the state dynamics.

set-up is selected based on the trained NN. The concept offers a significant improvement of the integration (and thus estimation) performance with rather a negligible impact on the computational complexity and allow accuracy assessment of the IR error estimate. Although the integration error estimation was discussed in the state estimation and prediction, it can be directly applied to any problem where the integral relations are solved numerically.

REFERENCES

- Alsadi, N., Gadsden, S.A., and Yawney, J. (2023). Intelligent estimation: A review of theory, applications, and recent advances. *Digital Signal Processing*, 135, 103966.
- Anderson, B.D.O. and Moore, J.B. (1979). *Optimal Filtering*. Prentice Hall, New Jersey.
- Anthony, R. and Rabinowitz, P. (1978). *A First Course in Numerical Analysis: Second Edition*. Dover Publications.
- Bao, Y., Velni, J.M., Basina, A., and Shahbakhti, M. (2020). Identification of state-space linear parameter-varying models using artificial neural networks. *IFAC-PapersOnLine*, 53, 5286—5291.
- Bergman, N. (1999). *Recursive Bayesian Estimation: Navigation and Tracking Applications*. Ph.D. thesis, Linköping University, Sweden.
- Chen, X., Särkkä, S., and Godsill, S. (2015). A bayesian particle filtering method for brain source localisation. *Digital Signal Processing*, 47, 192–204. Special Issue in Honour of William J. (Bill) Fitzgerald.
- Closas, P., Fernandez-Prades, C., and Fernandez-Rubio, J.A. (2009). A bayesian approach to multipath mitigation in gns receivers. *IEEE Journal of Selected Topics in Signal Processing*, 3(4), 695–706.
- Doucet, A., De Freitas, N., and Gordon, N. (eds.) (2001). *Sequential Monte Carlo Methods in Practice*. Springer. (Ed. Doucet A., de Freitas N., and Gordon N.).
- Duník, J., Soták, M., Veselý, M., Straka, O., and Hawkinson, W.J. (2019). Design of Rao-Blackwellised point-mass filter with application in terrain aided navigation. *IEEE Transactions on Aerospace and Electronic Systems*, 55(1), 251–272.
- Duník, J., Straka, O., Šimandl, M., and Blasch, E. (2015). Random-point-based filters: Analysis and comparison in target tracking. *IEEE Transactions on Aerospace and Electronic Systems*, 51(2), 303–308.
- Duník, J., Straka, O., Matoušek, J., and Blasch, E. (2022). Copula-based convolution for fast point-mass prediction. *Signal Processing*, 192, 108367.
- Gorji, A. and Menhaj, M. (2008). Identification of nonlinear state space models using an MLP network trained by the EM algorithm. In *2008 IEEE International Joint Conference on Neural Networks (IEEE World Congress on Computational Intelligence)*, 53–60.
- Haykin, S. (1999). *Neural Networks: A comprehensive foundation*. Prentice-Hall, Upper Saddle River, NJ, 2nd edition.
- Heo, S. and Lee, J.H. (2018). Fault detection and classification using artificial neural networks. *IFAC-PapersOnLine*, 51(18), 470–475.
- Herman, E. and Strang, G. (2017). *Calculus Volume 2*. OpenStax.
- Jeon, H.C., Park, W.J., and Park, C.G. (2018). Grid design for efficient and accurate point mass filter-based terrain referenced navigation. *IEEE Sensors Journal*, 18(4), 1731–1738.
- Julier, S.J. and Uhlmann, J.K. (2004). Unscented filtering and nonlinear estimation. *IEEE Proceedings*, 92(3), 401–421.
- Lindfors, M., Hendeby, G., Gustafsson, F., and Karlsson, R. (2016). Vehicle speed tracking using chassis vibrations. In *2016 IEEE Intelligent Vehicles Symposium*. Gothenburg, Sweden.
- Lloyd, S., Irani, R.A., and Ahmadi, M. (2020). Using neural networks for fast numerical integration and optimization. *IEEE Access*, 8, 84519–84531.
- Miller, J.C.P. (1960). Numerical quadrature over a rectangular domain in two or more dimensions: Part 1. quadrature over a square, using up to sixteen equally spaced points. *Mathematics of Computation*, 14(69), 13–20.
- Press, W.H., Teukolsky, S.A., Vetterling, W.T., and Flannery, B.P. (2007). *Numerical Recipes 3rd Edition: The Art of Scientific Computing*. Cambridge University Press, 3 edition.
- Saravanan, R. and Sujatha, P. (2018). A state of art techniques on machine learning algorithms: A perspective of supervised learning approaches in data classification. In *2018 Second International Conference on Intelligent Computing and Control Systems (ICICCS)*, 945–949. doi:10.1109/ICCONS.2018.8663155.
- Särkkä, S. (2013). *Bayesian Filtering and Smoothing*. Cambridge University Press.
- Schoukens, M. (2021). Improved initialization of state-space artificial neural networks. *arXiv preprint arXiv:2103.14516*.
- Shaukat, N., Ali, A., Iqbal, M., Moinuddin, M., and Otero, P. (2021). Multi-sensor fusion for underwater vehicle localization by augmentation of RBF neural network and error-state Kalman filter. *Sensors*, 21, 1149.
- Stoer, J., Bartels, R., Gautschi, W., Bulirsch, R., and Witzgall, C. (2002). *Introduction to Numerical Analysis*. Texts in Applied Mathematics. Springer New York.
- Stroud, A.H. (1971). *Approximate calculation of multiple integrals*. Prentice-Hall Englewood Cliffs, NJ.
- Tian, G., Zhou, Q., Birari, R., Qi, J., and Qu, Z. (2020). A hybrid-learning algorithm for online dynamic state estimation in multimachine power systems. *IEEE Transactions on Neural Networks and Learning Systems*, 31(12), 5497–5508.
- Šimandl, M. and Duník, J. (2009). Derivative-free estimation methods: New results and performance analysis. *Automatica*, 45(7), 1749–1757.
- Šimandl, M., Královec, J., and Söderström, T. (2006). Advanced point-mass method for nonlinear state estimation. *Automatica*, 42(7), 1133–1145.
- Yoon, B. (2021). A machine learning approach for efficient multi-dimensional integration. *Scientific Reports*, 11, 18965.
- Zhai, B., Yi, W., Li, M., Ju, H., and Kong, L. (2019). Data-driven XGBoost-based filter for target tracking. *The Journal of Engineering*, 2019(20), 6683–6687.
- Zhe-Zhao, Z., Yao-Nan, W., and Hui, W. (2006). Numerical integration based on a neural network algorithm. *Computing in Science and Engineering*, 8(4), 42–48.
- Zwillinger, D. (2003). *CRC Standard Mathematical Tables and Formulae*. CRC Press.